Electronic Supplementary Material (ESI) for Polymer Chemistry.
This journal is © The Royal Society of Chemistry 2023

# SUPPORTING INFORMATION

## *Synthesis of poly(ethylene glycol)-co-poly(caprolactone) di- and triblock copolymers and effect of architecture, dispersity and end-functionalisation on their aqueous self-assembly*

Karolis Norinkevicius[1,2], Jeppe Madsen[1], Line Elmstrøm Christiansen[2], Sebastian Meier[4], Andreas Horner[5], Radosław Górecki[6,7], Torsten Høybye Bak Regueira[2], Anders Egede Daugaard[1]

[1]Department of Chemical and Biochemical Engineering, Technical University of Denmark, Søltofts Plads 227, 2800 Kongens Lyngby, Denmark

[2]Deep Tech Center, Aquaporin A/S, Nymøllevej 78, 2800 Kongens Lyngby, Denmark

[4]Department of Chemistry, Technical University of Denmark, Kemitorvet 207, 2800 Kongens Lyngby, Denmark

[5]Institute of Biophysics, Johannes Kepler University Linz, Gruberstrasse 40, Linz, 4020, Austria

[6]Environmental Science and Engineering Program, Biological and Environmental Science and Engineering Division, King Abdullah University of Science and Technology (KAUST), 23955-6900 Thuwal, Saudi Arabia

[7]Advanced Membranes and Porous Materials Center, King Abdullah University of Science and Technology (KAUST), 23955-6900 Thuwal, Saudi Arabia

# 1 Size-exclusion chromatography (SEC)

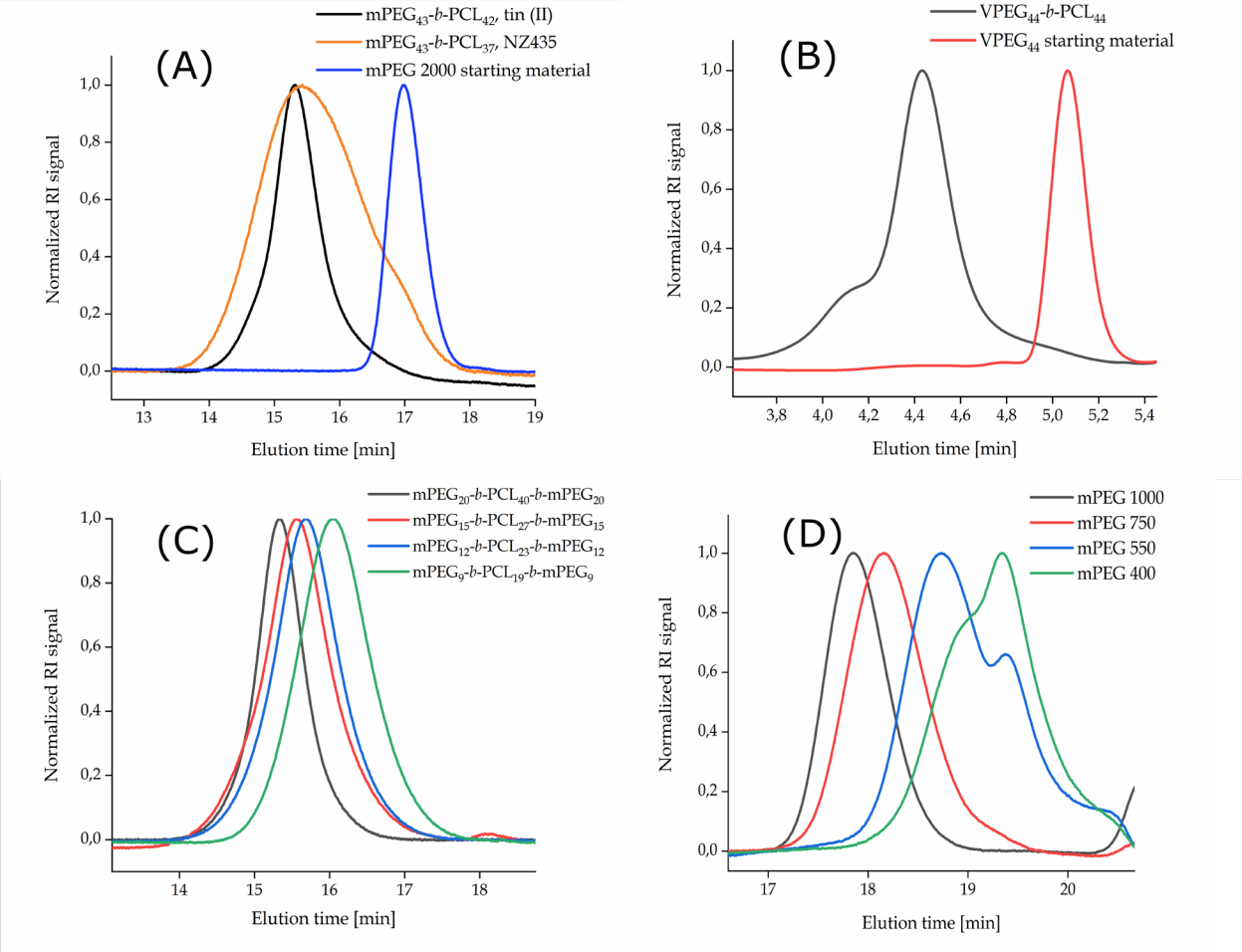


Figure S1.1 Size-exclusion chromatograms of (A) mPEG-*b*-PCL diblock copolymers prepared by enzymatic and chemocatalytic approach, including starting material of mPEG ($M_n$ ~ 2000), (B) vinyl terminated PEG-*b*-PCL and vinyl terminated PEG (35-50 EO) starting material, (C) mPEG-*b*-PCL-*b*-mPEG triblocks and their corresponding mPEG starting materials (D)

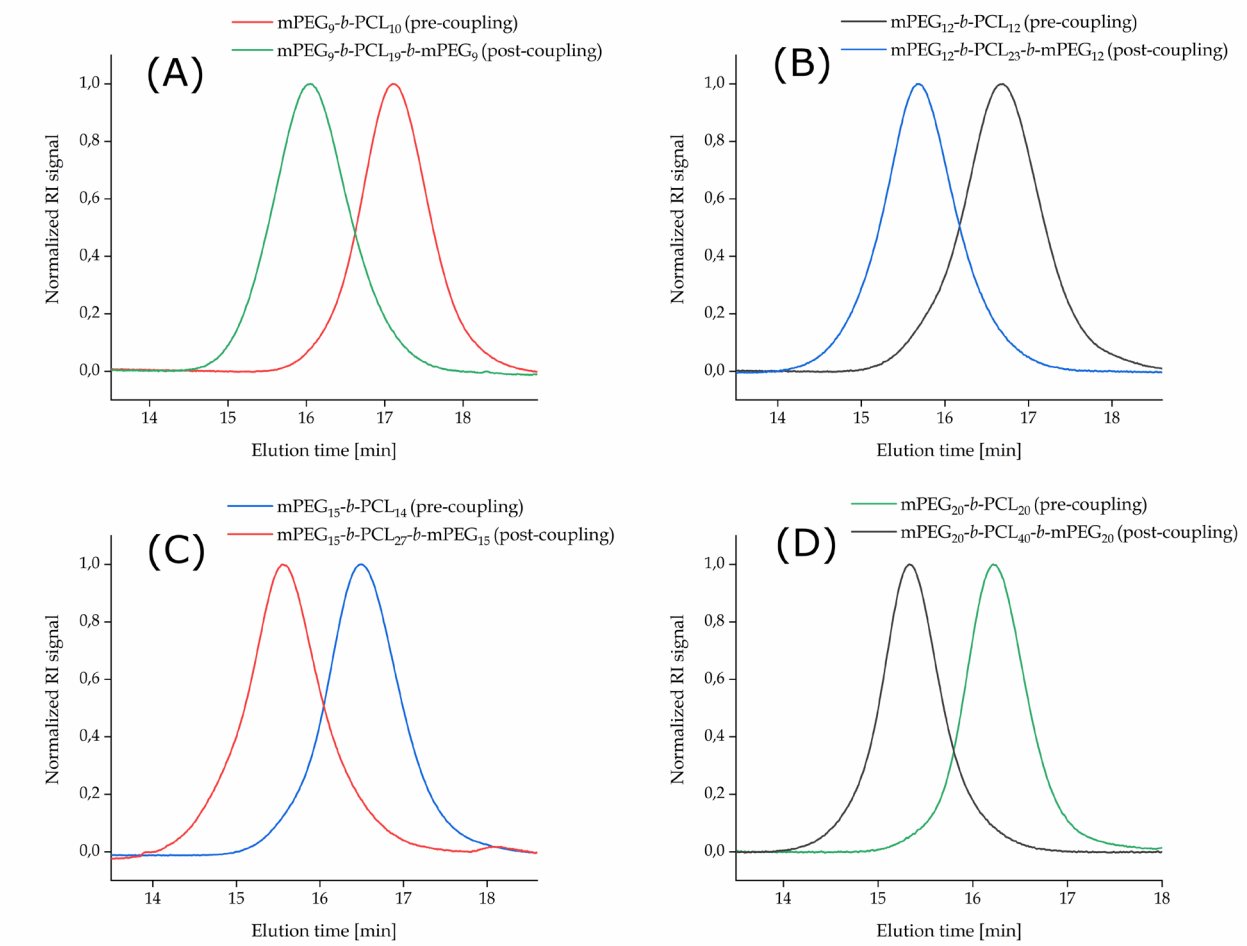


Figure S1.2 Size-exclusion chromatograms (A)-(D) showing mPEG-*b*-PCL diblock copolymers before coupling with hexamethylene diisocyanate (HMDI) and corresponding mPEG-*b*-PCL-*b*-mPEG triblock copolymers after the coupling reaction. The mPEG-*b*-PCL diblock copolymers were analyzed directly from the crude mixture (before addition of the HMDI). The mPEG-*b*-PCL-*b*-mPEG triblock copolymers were purified by fractional precipitation in diethyl ether before the analysis

# 2 $^{1}$H Nuclear magnetic resonance (NMR) spectroscopy

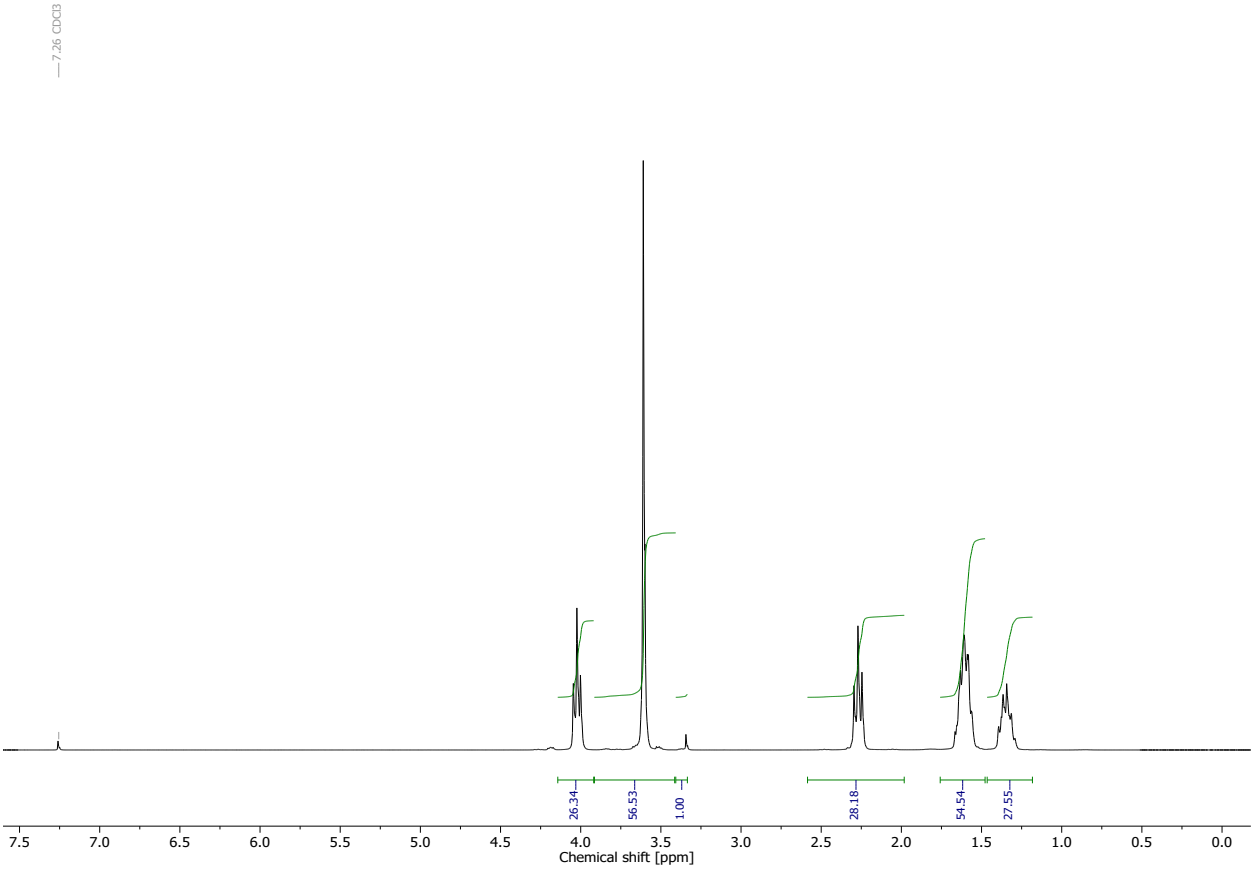


Figure S2.1 $^{1}$H NMR spectrum of mPEG$_{43}$-*b*-PCL$_{42}$ diblock copolymer synthesized by tin (II) catalyzed pathway

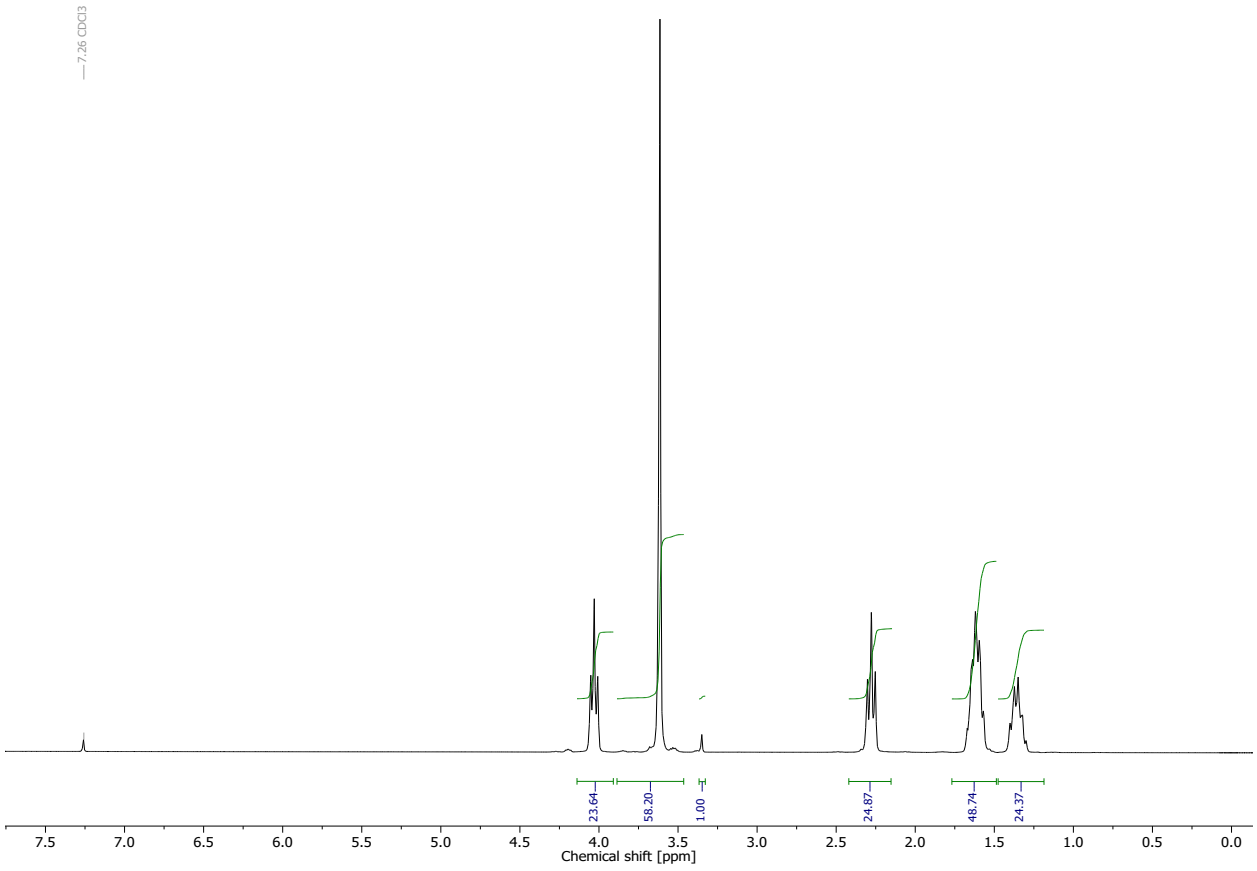


Figure S2.2 $^{1}$H NMR spectrum of mPEG$_{43}$-*b*-PCL$_{37}$ diblock copolymer synthesized by enzymatically catalyzed pathway

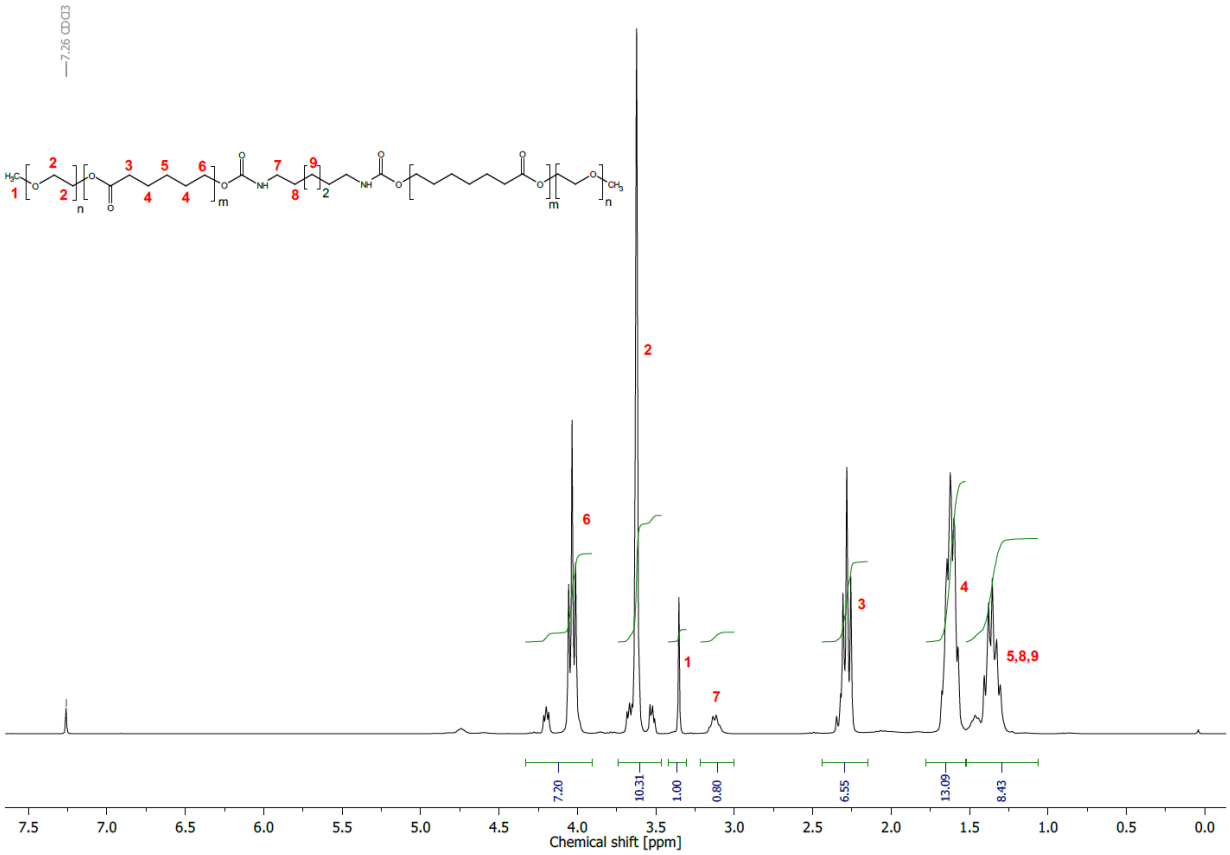


Figure S2.3 $^{1}$H NMR spectrum of mPEG$_9$-*b*-PCL$_{19}$-*b*-mPEG$_9$ triblock copolymer

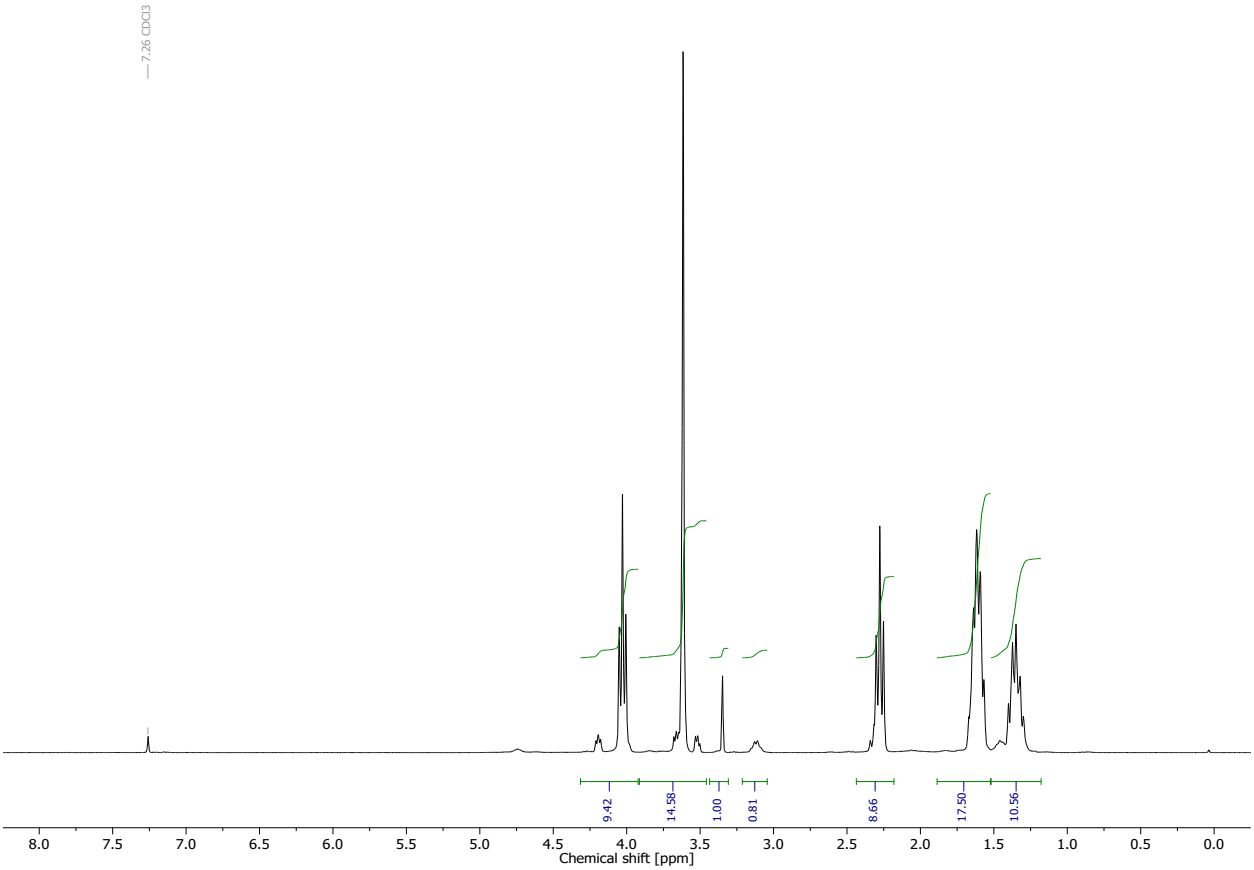


Figure S2.4 $^{1}$H NMR spectrum of mPEG$_{12}$-*b*-PCL$_{23}$-*b*-mPEG$_{12}$ triblock copolymer

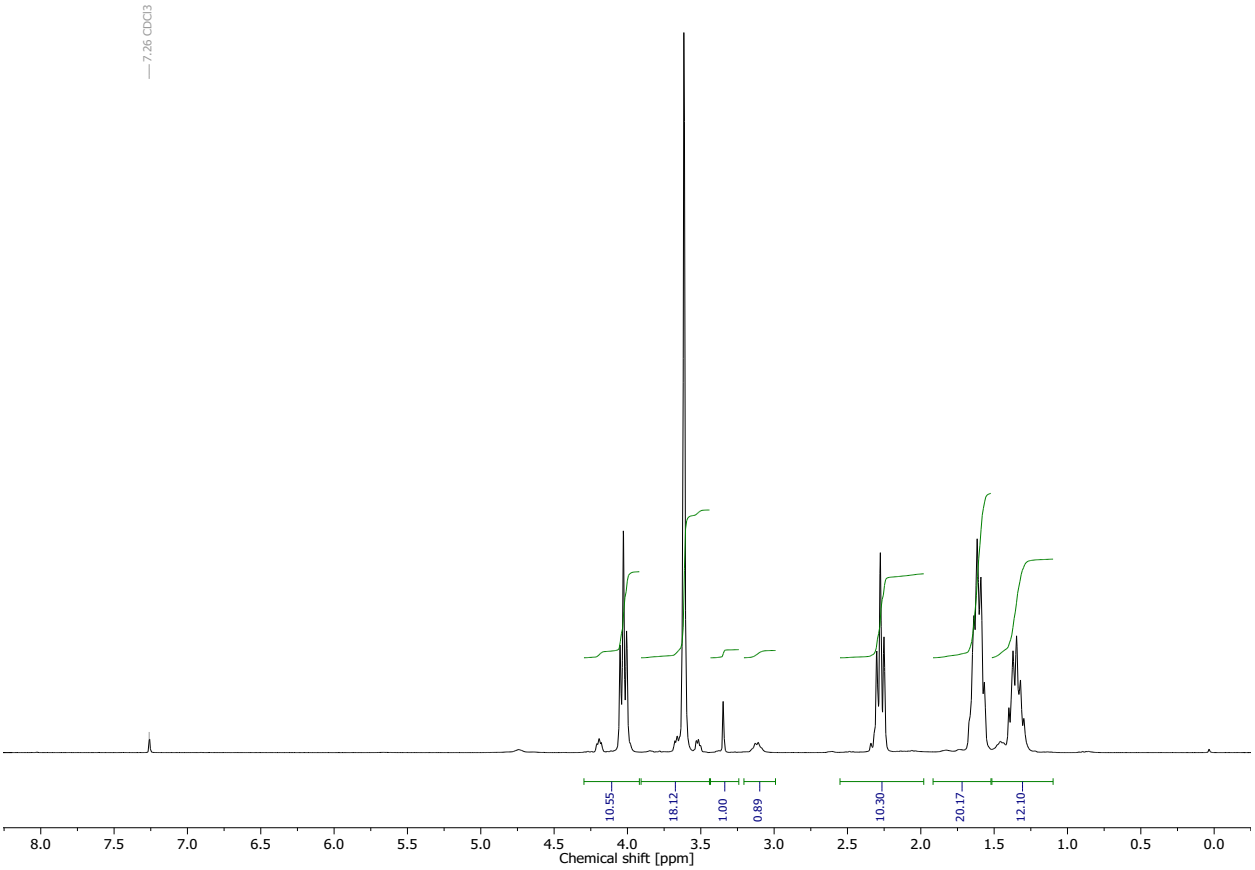


Figure S2.5 $^{1}$H NMR spectrum of mPEG$_{15}$-*b*-PCL$_{27}$-*b*-mPEG$_{15}$ triblock copolymer

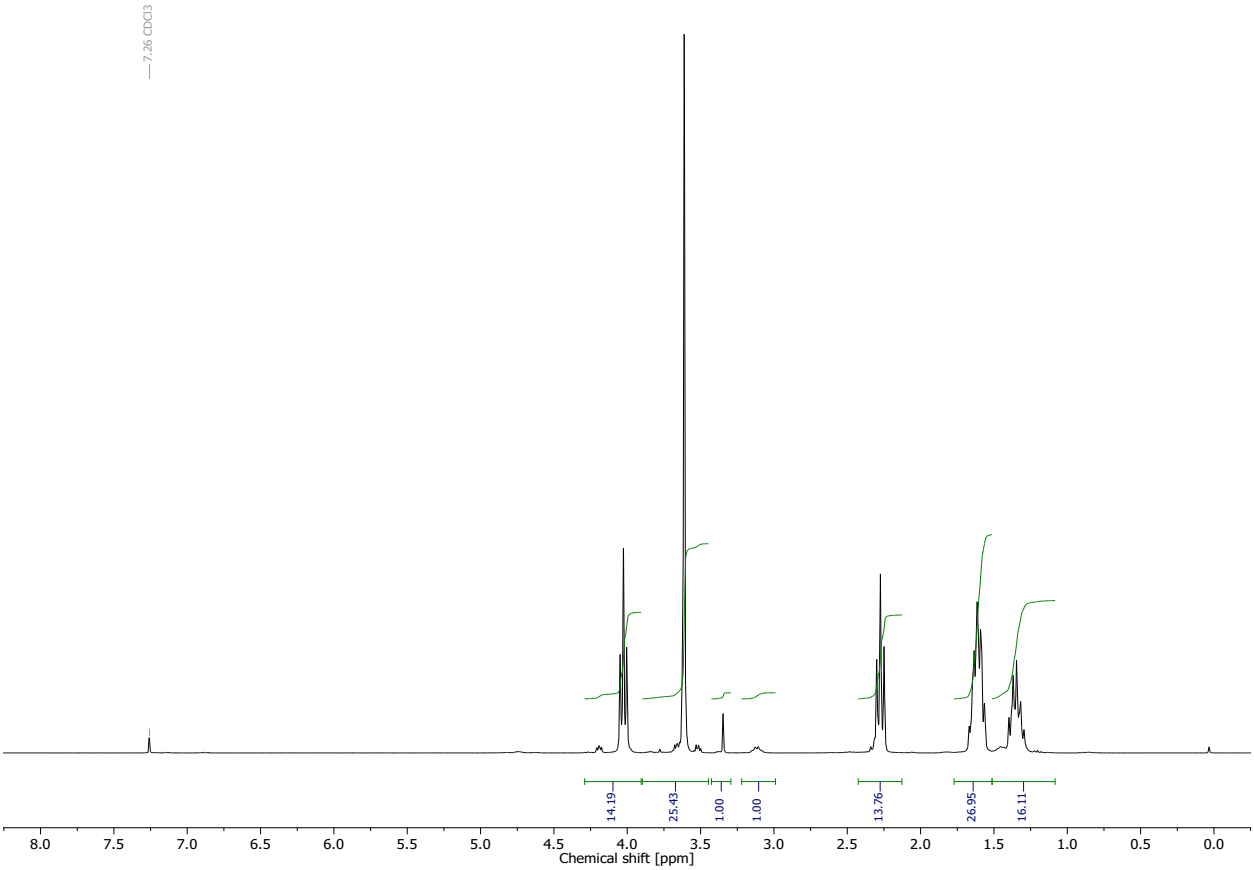


Figure S2.6 $^{1}$H NMR spectrum of mPEG$_{20}$-*b*-PCL$_{40}$-*b*-mPEG$_{20}$ triblock copolymer

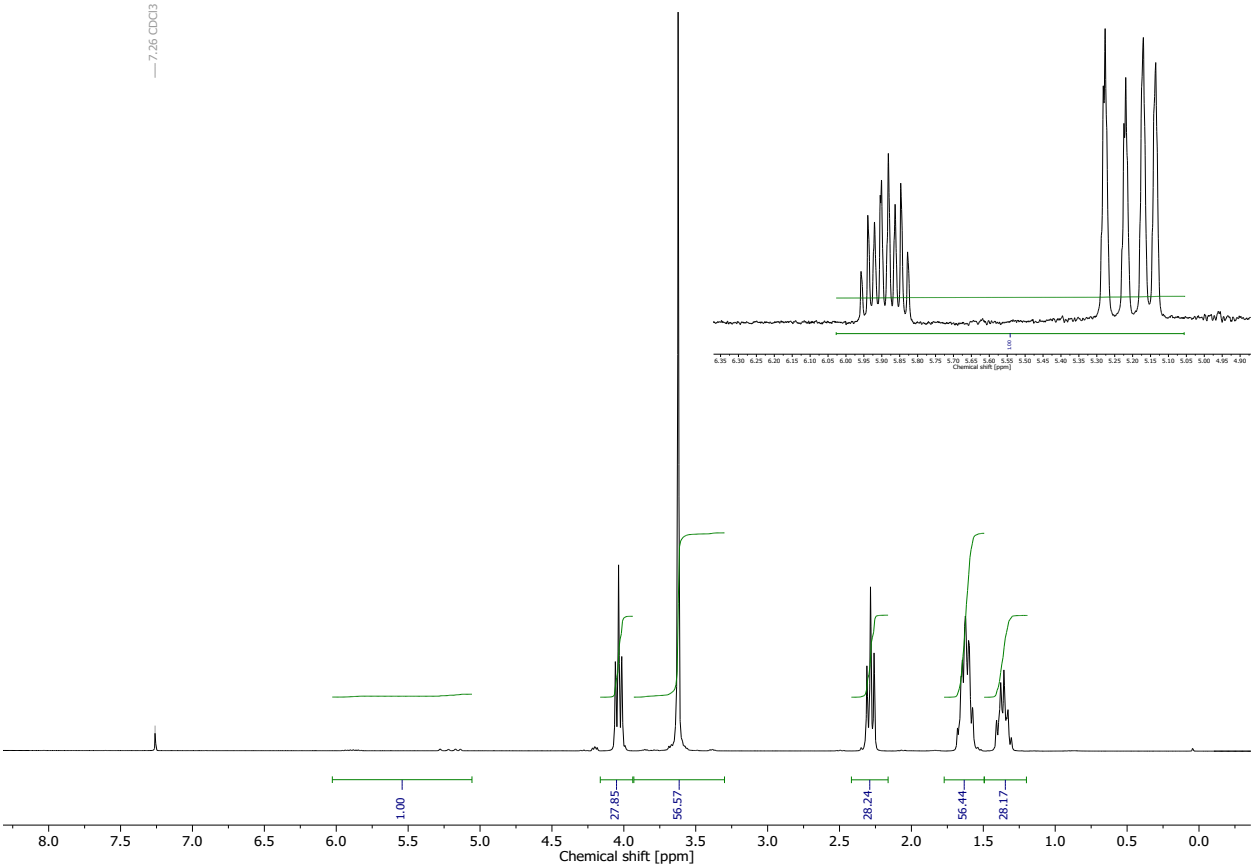


Figure S2.7 $^{1}$H NMR spectrum of vinyl terminated $PEG_{42}$-*b*-$PCL_{42}$ diblock copolymer, top right corner showcasing vinyl terminal groups

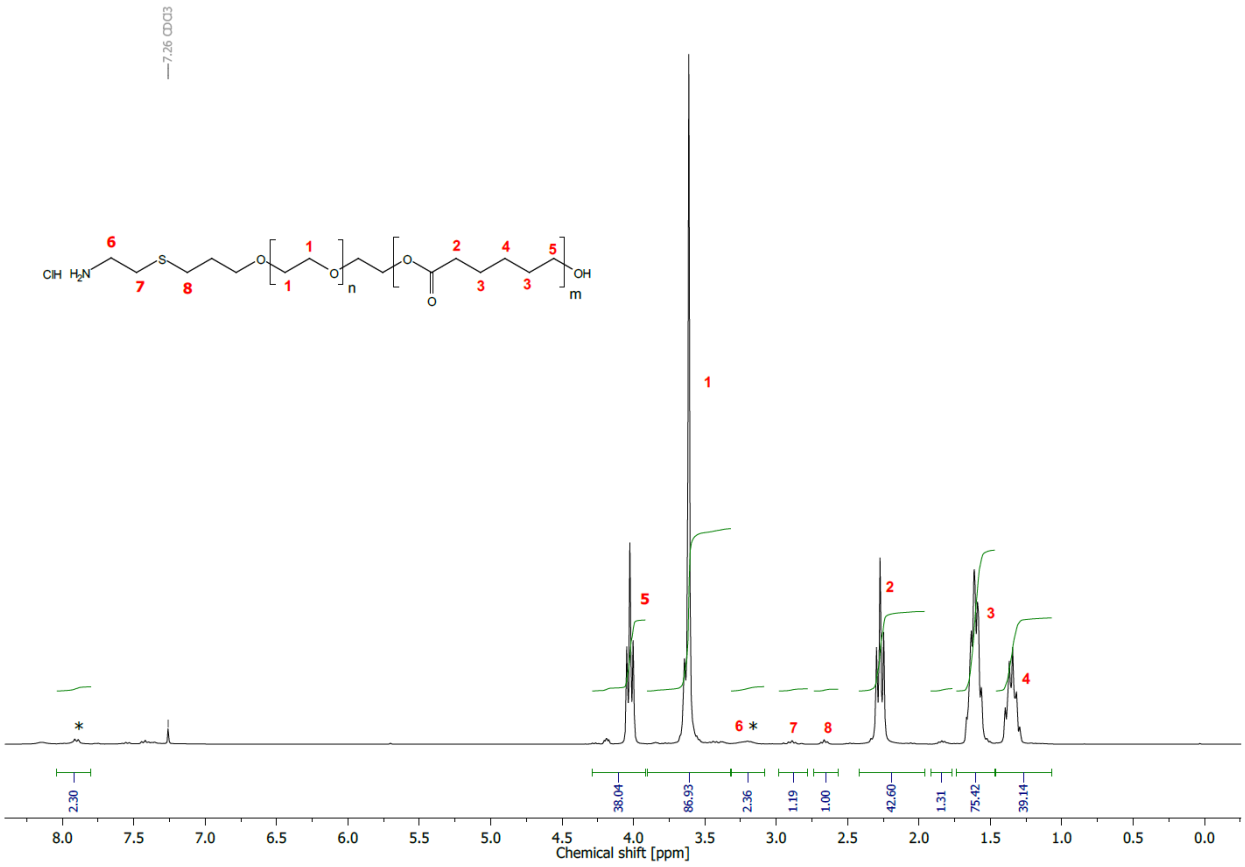


Figure S2.8 $^{1}$H NMR spectrum of HCl.$NH_2$-$PEG_{43}$-*b*-$PCL_{43}$ diblock copolymer. *solvent residues

# 3 $^{13}$C NMR time-series measurements

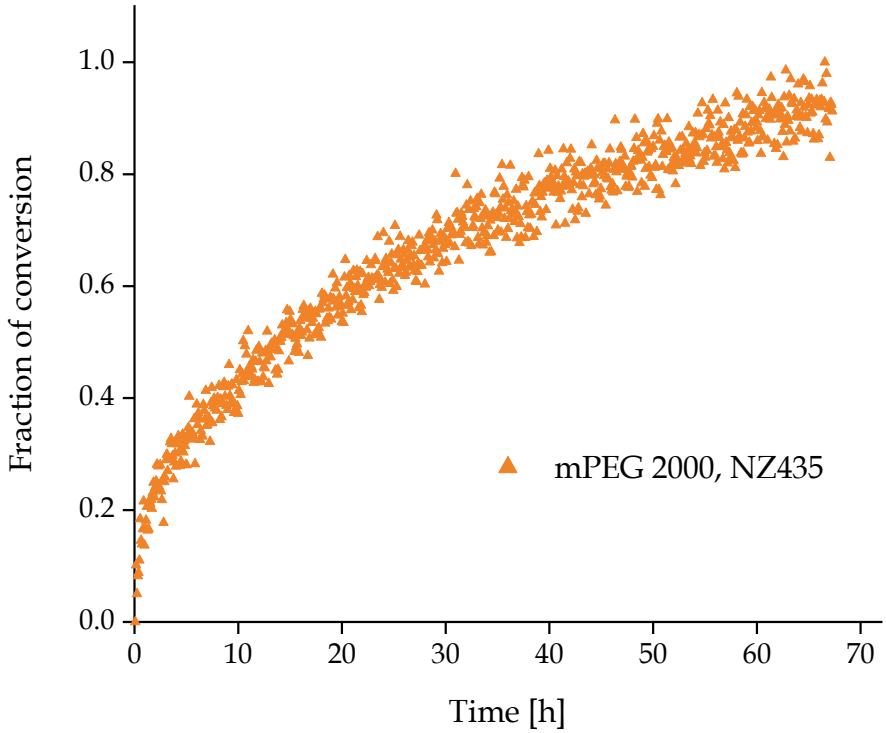


Figure S3.1 Extended $^{13}$C NMR time-series measurements of ε-caprolactone conversion over time for lipase (NZ435) catalyzed ring-opening polymerization

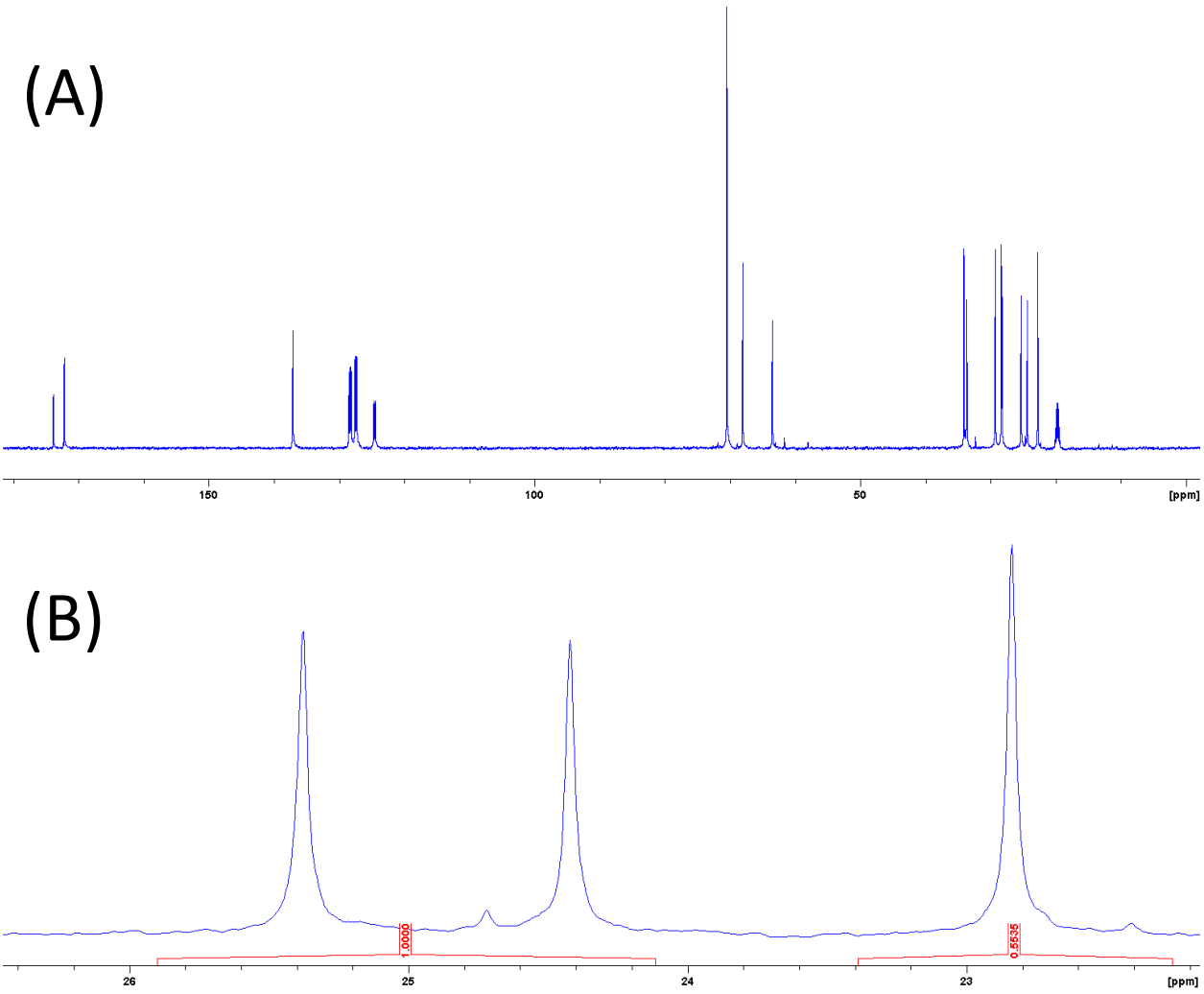


Figure S3.2 An example of $^{13}C$ NMR spectra for the tin (II) catalyzed reaction. The spectra were obtained from 2D fourier transformation of the free induction decay (FID, 50$^{th}$ time point). (A) Displays zoomed out $^{13}C$ NMR spectrum, while (B) shows zoomed in region of the integration. Toluene-d8 was used as the solvent

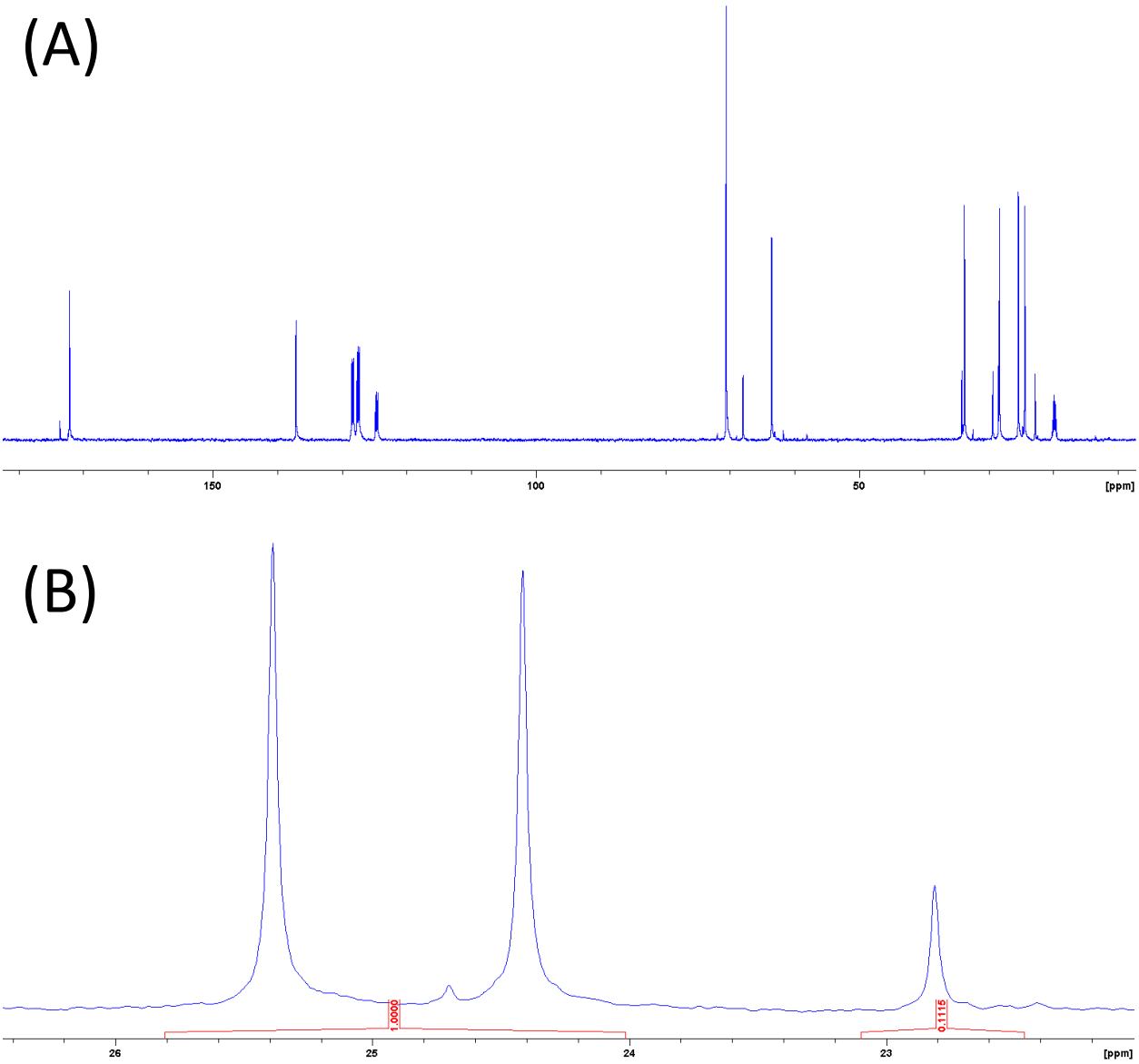


Figure S3.3 An example of $^{13}C$ NMR spectra for the tin (II) catalyzed reaction. The spectra were obtained from 2D fourier transformation of the free induction decay (FID, 100$^{th}$ time point). (A) Displays zoomed out $^{13}C$ NMR spectrum, while (B) shows zoomed in region of the integration. Compared to the Figure S3.2 it can be seen that the intensity of the signal between 26 and 24 ppm is increasing in relation to the signal between 23 and 22 ppm indicating growth of poly(caprolactone) chain and consumption of the monomer of caprolactone, respectively. Toluene-d8 was used as the solvent

# 4 Fourier-transform infrared spectroscopy (FT-IR)

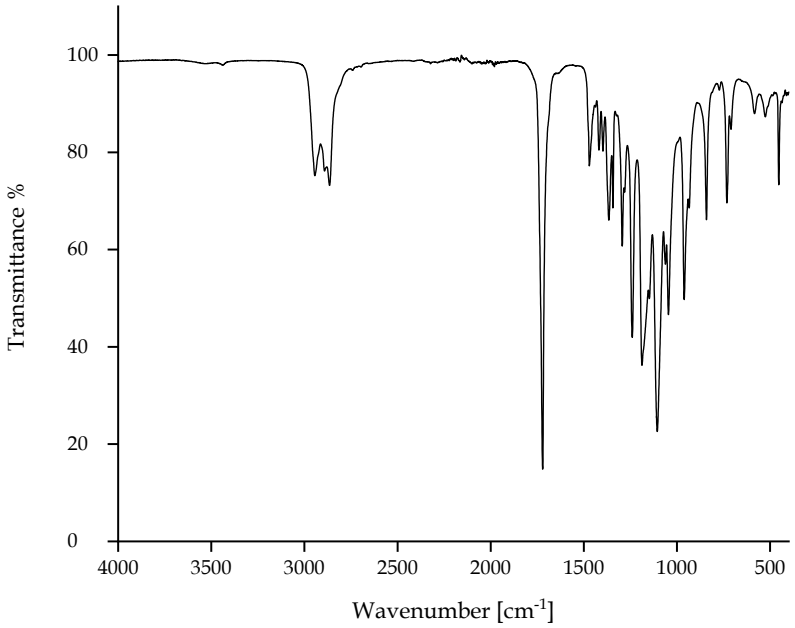


Figure S4.1 FT-IR spectrum of $mPEG_{43}$-*b*-$PCL_{42}$ diblock copolymer synthesized by tin (II) catalyzed pathway

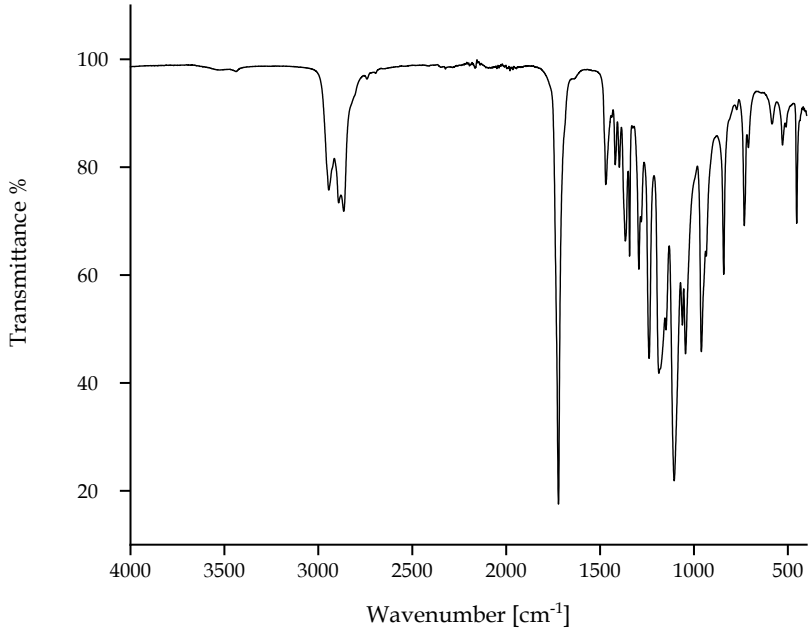


Figure S4.2 FT-IR spectrum of $mPEG_{43}$-*b*-$PCL_{37}$ diblock copolymer synthesized by enzymatically catalyzed pathway

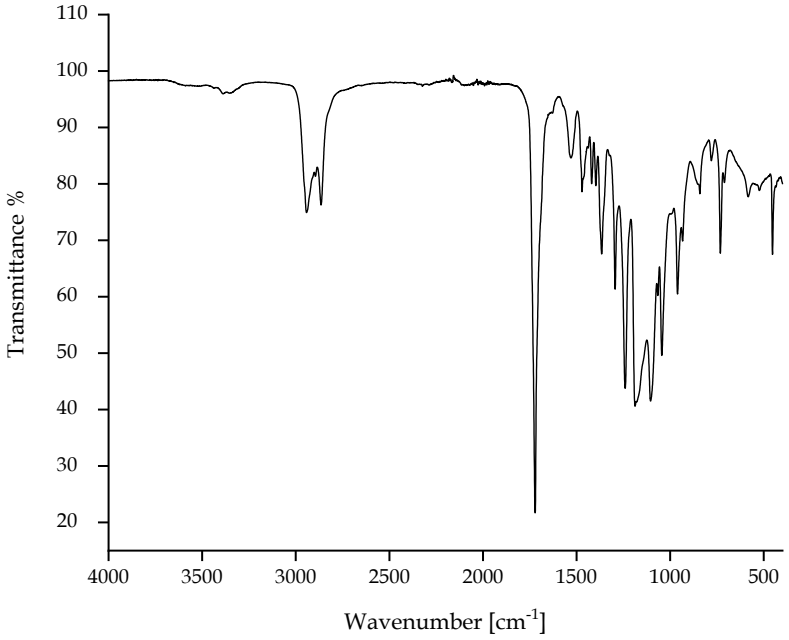


Figure S4.3 FT-IR spectrum of $mPEG_9$-*b*-$PCL_{19}$-*b*-$mPEG_9$ triblock copolymer

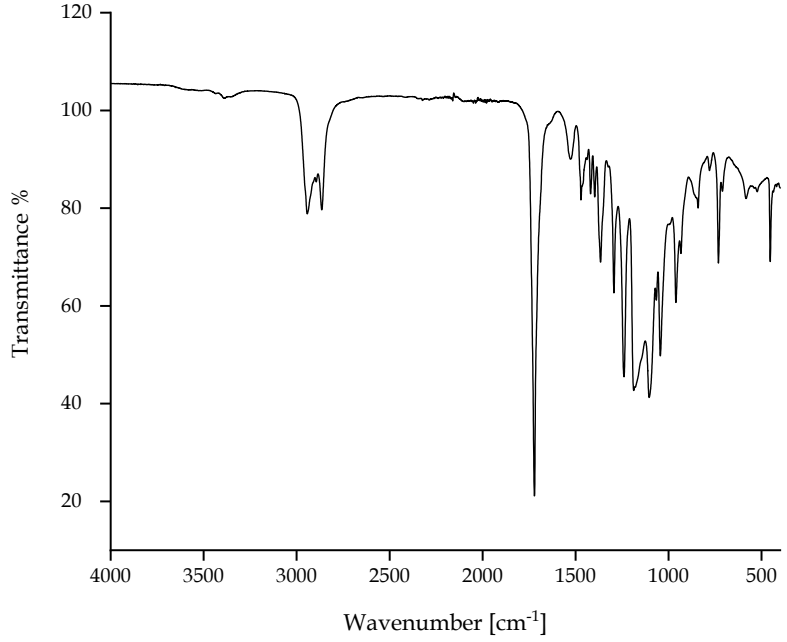


Figure S4.4 FT-IR spectrum of $mPEG_{12}$-*b*-$PCL_{23}$-*b*-$mPEG_{12}$ triblock copolymer

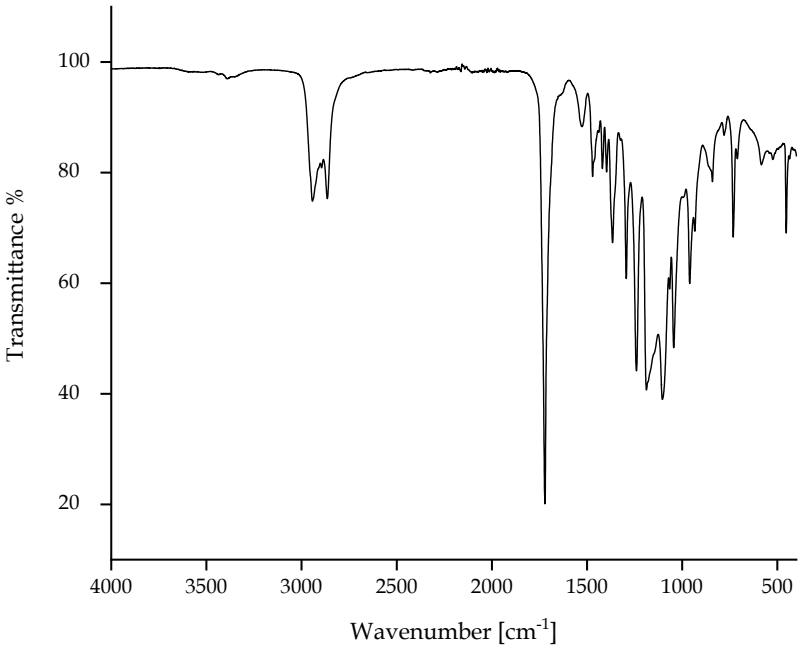


Figure S4.5 FT-IR spectrum of $mPEG_{15}$-*b*-$PCL_{27}$-*b*-$mPEG_{15}$ triblock copolymer

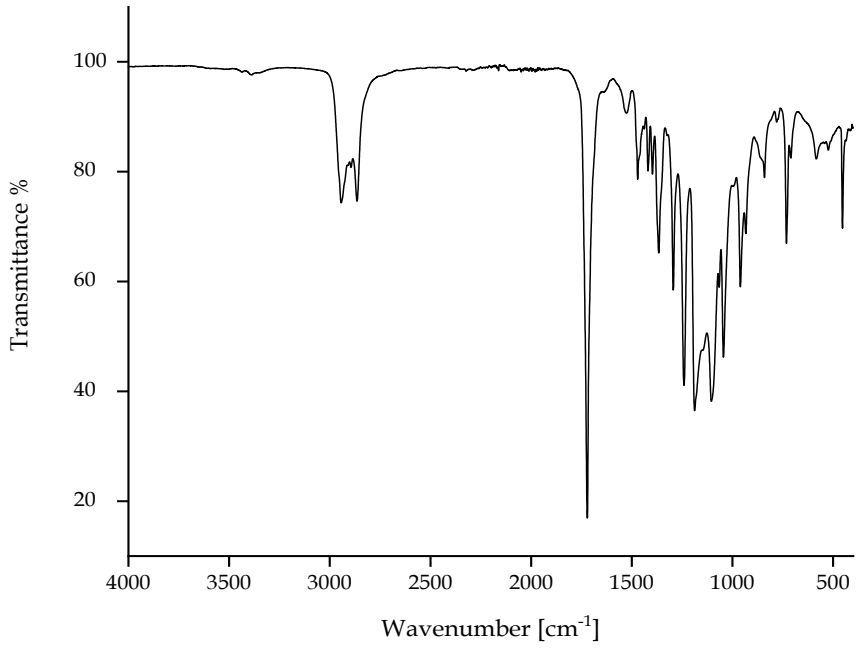


Figure S4.6 FT-IR spectrum of $mPEG_{20}$-*b*-$PCL_{40}$-*b*-$mPEG_{20}$ triblock copolymer

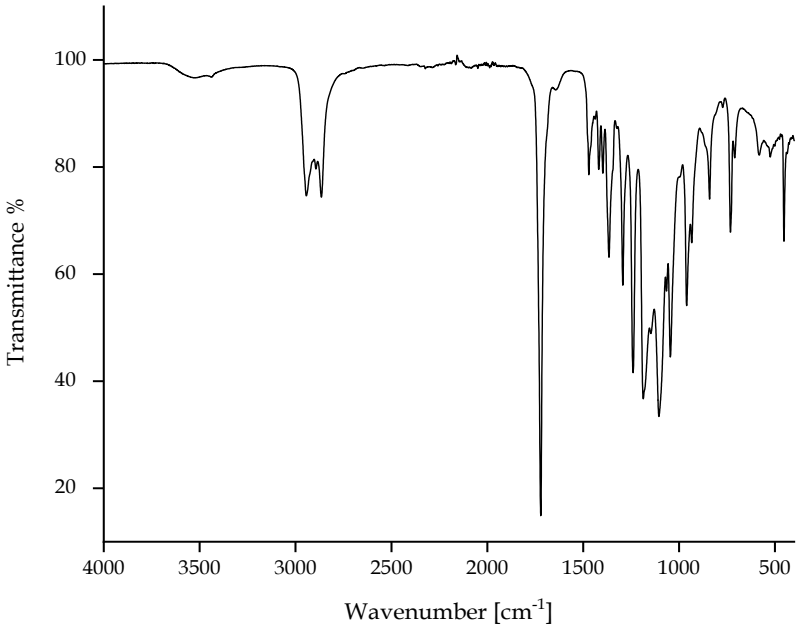


Figure S4.7 FT-IR spectrum of vinyl terminated $PEG_{42}$-*b*-$PCL_{42}$ diblock copolymer

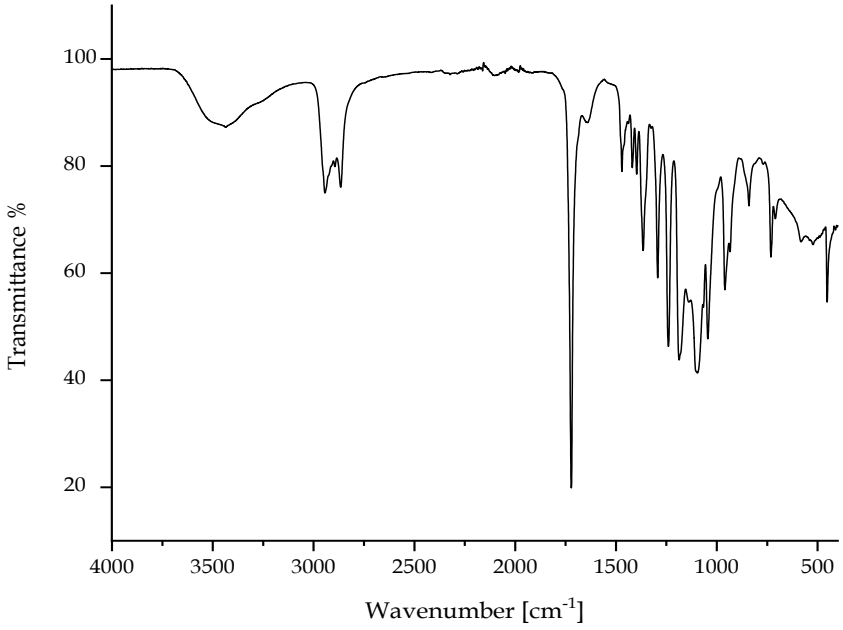


Figure S4.8 FT-IR spectrum of $NH_2$-$PEG_{43}$-*b*-$PCL_{43}$ diblock copolymer

# 5 Differential scanning calorimetry (DSC)

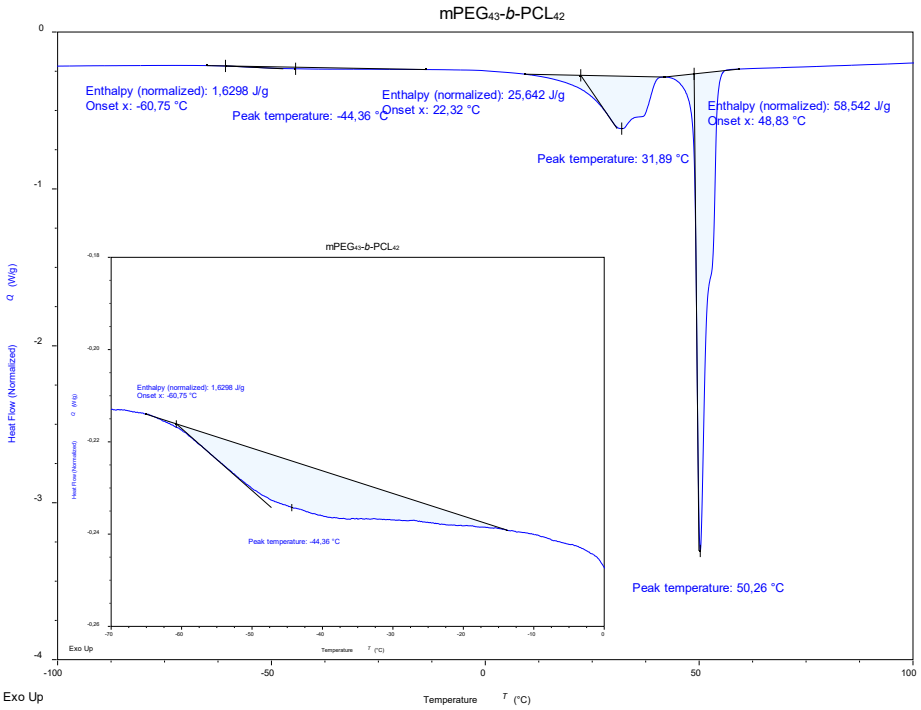


Figure S5.1 DSC curve of $mPEG_{43}$-*b*-$PCL_{42}$ diblock copolymer synthesized by tin (II) catalyzed pathway. $T_g$ (mPEG) = -44.36 °C, $T_m$ (mPEG) = 31.89 °C, $T_m$ (PCL) = 50.26 °C

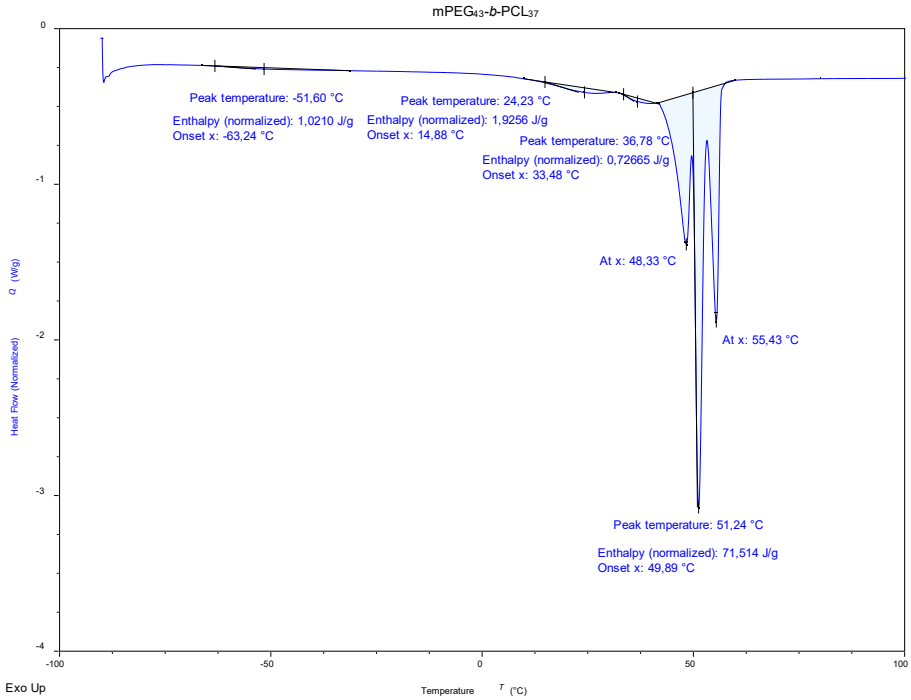


Figure S5.2 DSC curve of $mPEG_{43}$-*b*-$PCL_{37}$ diblock copolymer synthesized by enzymatically catalyzed pathway. $T_g$ (mPEG) = -51.60 °C, $T_{m1}$ (mPEG) = 24.23 °C, $T_{m2}$ (mPEG) = 36.78 °C, $T_{m1}$ (PCL) = 48.33 °C, $T_{m2}$ (PCL) = 51.24 °C, $T_{m3}$ = 55.43 °C

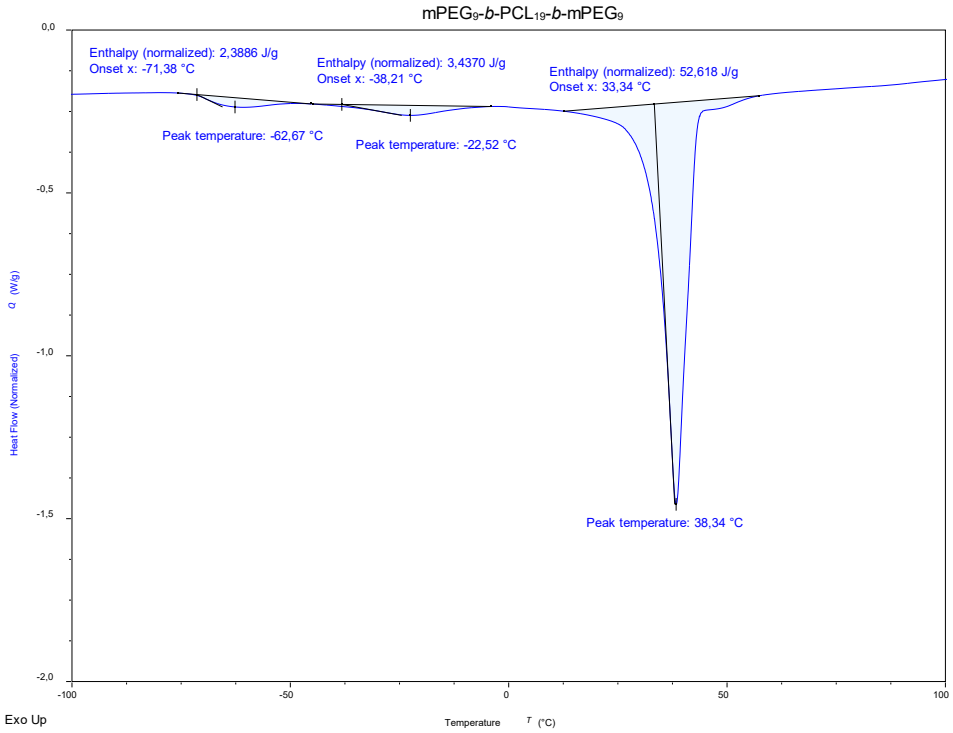


Figure S5.3 DSC curve of $mPEG_9$-*b*-$PCL_{19}$-*b*-$mPEG_9$ triblock copolymer. $T_g$ (mPEG) = -62.67 °C, $T_m$ (mPEG) = -22.52 °C, $T_m$ (PCL) = 38.34 °C

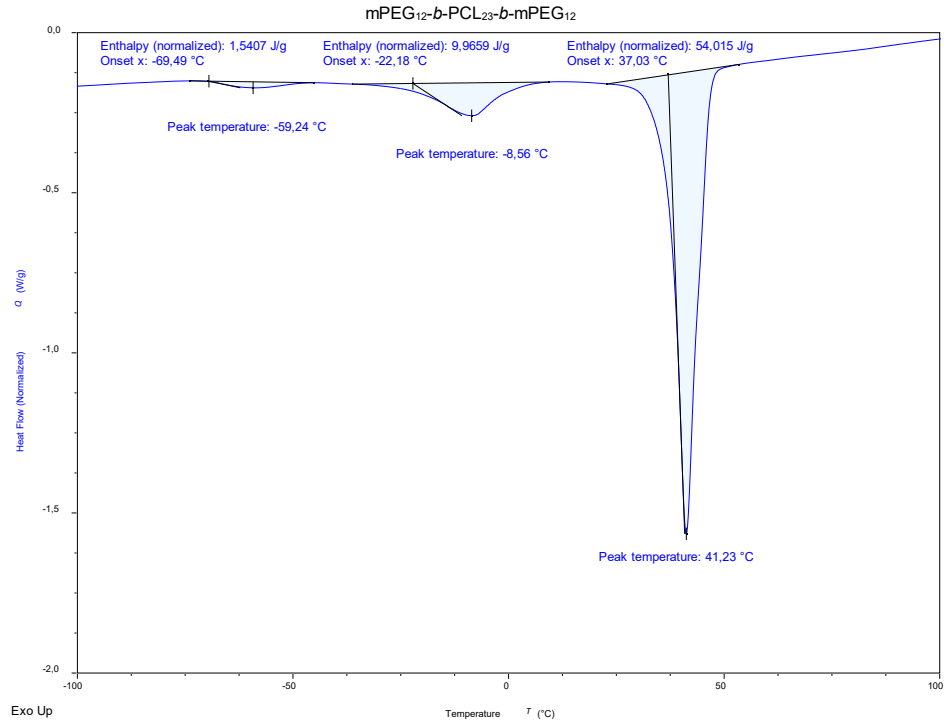


Figure S5.4 DSC curve of $mPEG_{12}$-*b*-$PCL_{23}$-*b*-$mPEG_{12}$ triblock copolymer. $T_g$ (mPEG) = -59.24 °C, $T_m$ (mPEG) = -8.56 °C, $T_m$ (PCL) = 41.23 °C

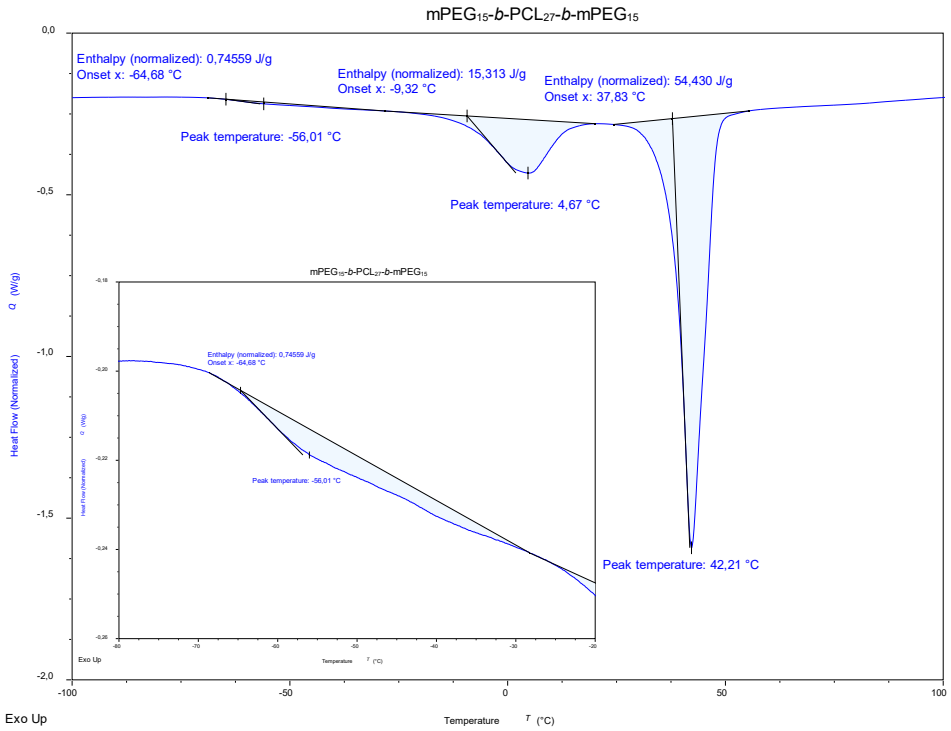


Figure S5.5 DSC curve of $mPEG_{15}$-*b*-$PCL_{27}$-*b*-$mPEG_{15}$ triblock copolymer. $T_g$ (mPEG) = -56.01 °C, $T_m$ (mPEG) = 4.67 °C, $T_m$ (PCL) = 42.21 °C

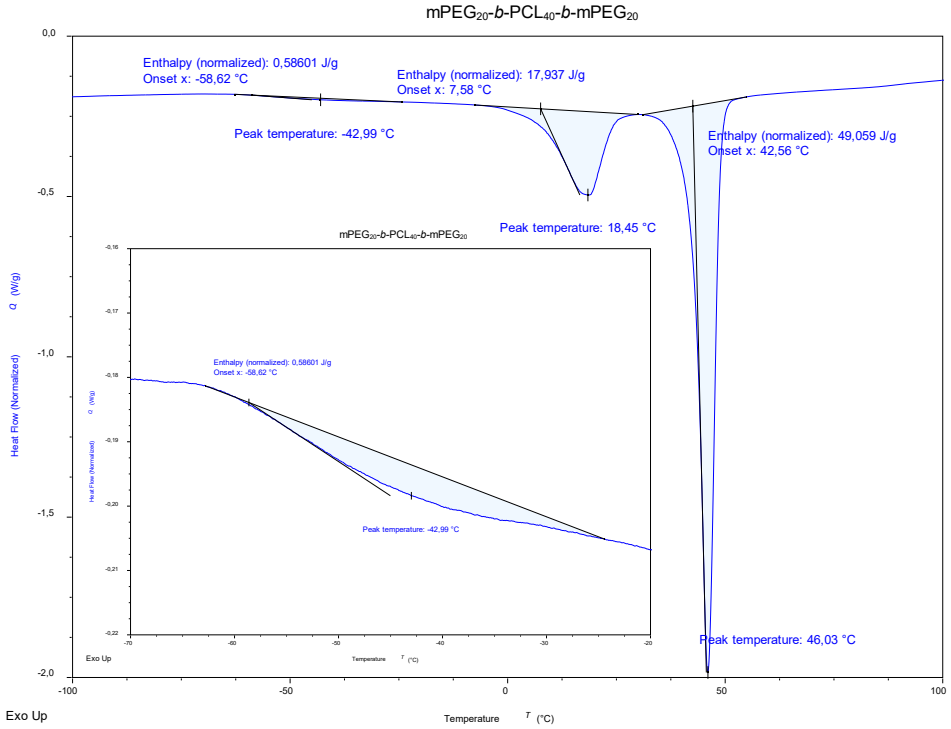


Figure S5.6 DSC curve of $mPEG_{20}$-*b*-$PCL_{40}$-*b*-$mPEG_{20}$ triblock copolymer. $T_g$ (mPEG) = -42.99 °C, $T_m$ (mPEG) = 18.45 °C, $T_m$ (PCL) = 46.03 °C

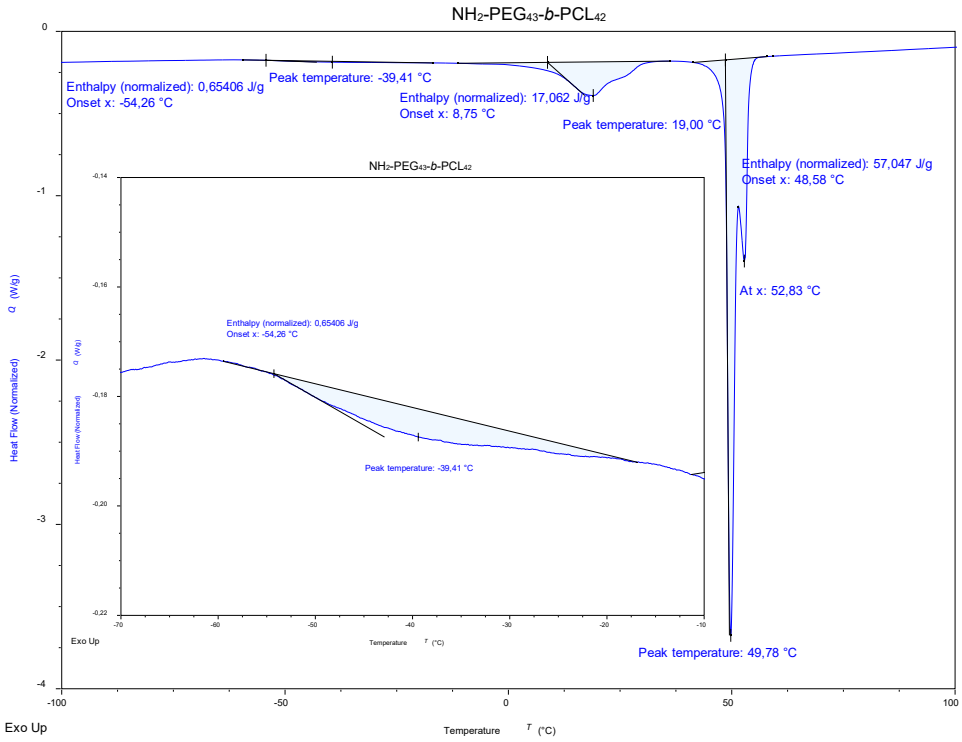


Figure S5.7 DSC curve of $NH_2$-$PEG_{43}$-*b*-$PCL_{43}$ diblock copolymer. $T_g$ (PEG) = -39.41 °C, $T_m$ (PEG) = 19 °C, $T_{m1}$ (PCL) = 49.78 °C, $T_{m2}$ = 52.83 °C

# 6 Cryogenic-transmission electron microscopy (Cryo-TEM)

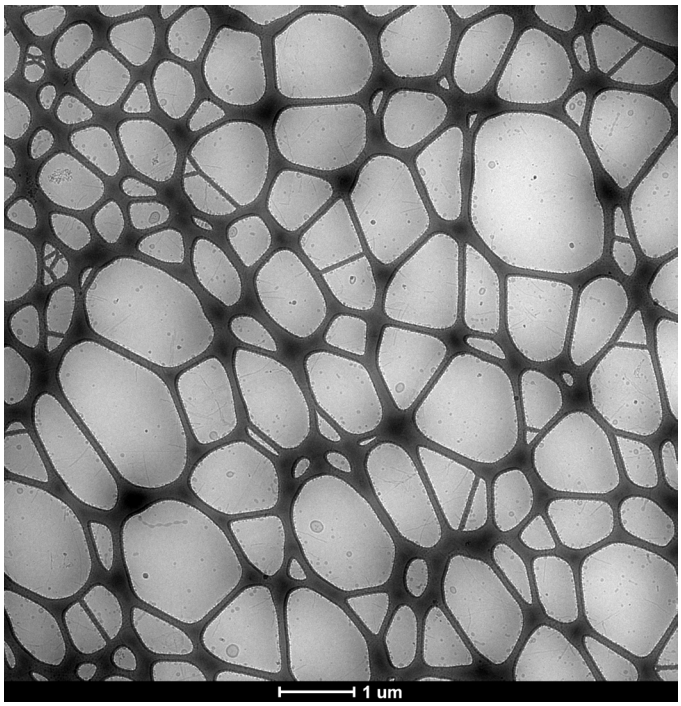


Figure S6.1 Cryo-TEM image of self-assembly suspension of $mPEG_{43}$-*b*-$PCL_{37}$ diblock copolymer synthesized by enzyme-catalyzed pathway

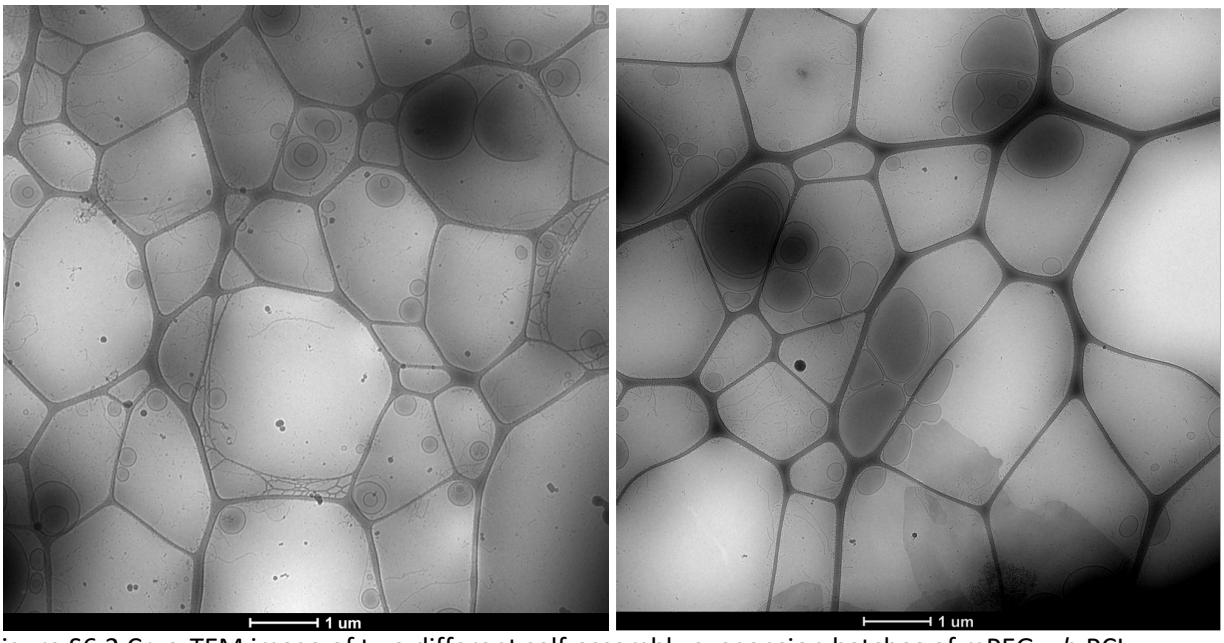


Figure S6.2 Cryo-TEM image of two different self-assembly suspension batches of $mPEG_{43}$-*b*-$PCL_{42}$ diblock copolymer synthesized by tin (II) catalyzed pathway

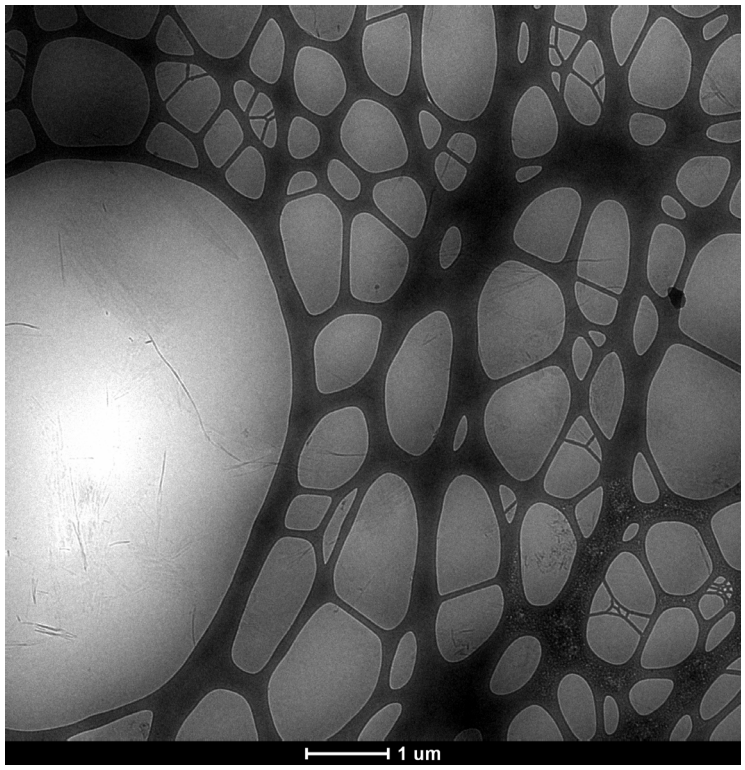


Figure S6.3 Cryo-TEM image of $mPEG_9$-*b*-$PCL_{19}$-*b*-$mPEG_9$ triblock copolymer self-assembly suspension

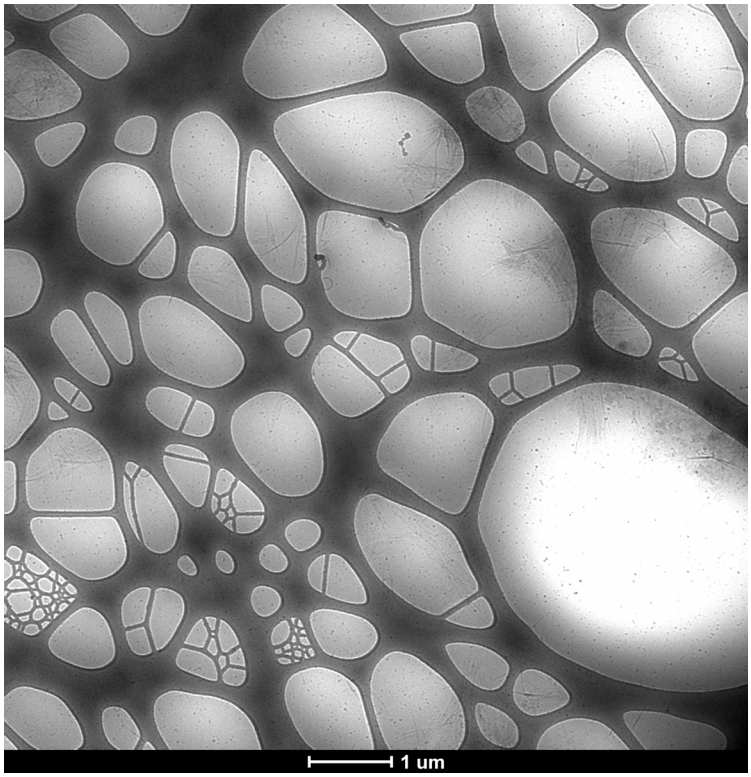


Figure S6.4 Cryo-TEM image of $mPEG_{12}$-*b*-$PCL_{23}$-*b*-$mPEG_{12}$ triblock copolymer self-assembly suspension

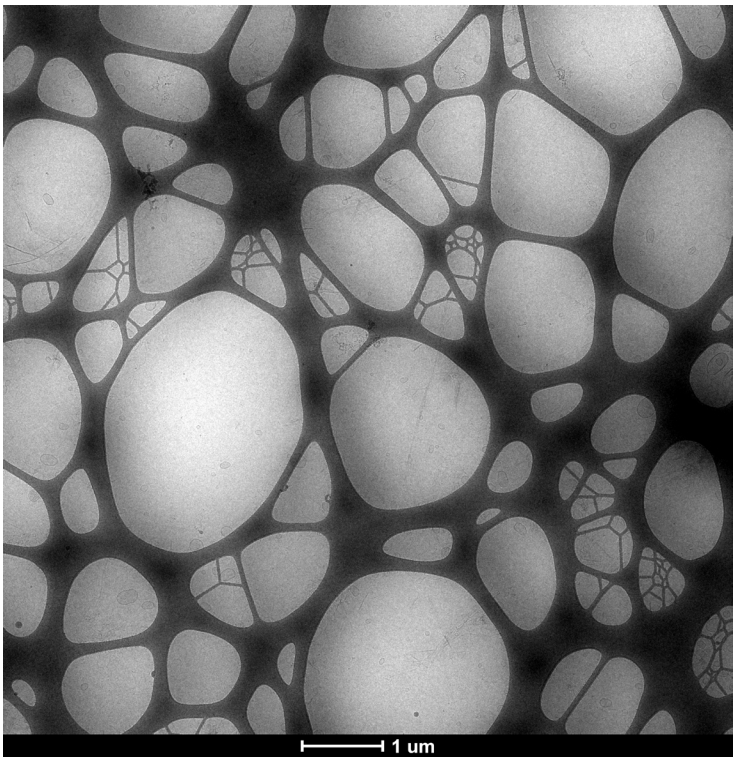


Figure S6.5 Cryo-TEM image of $mPEG_{15}$-*b*-$PCL_{27}$-*b*-$mPEG_{15}$ triblock copolymer self-assembly suspension

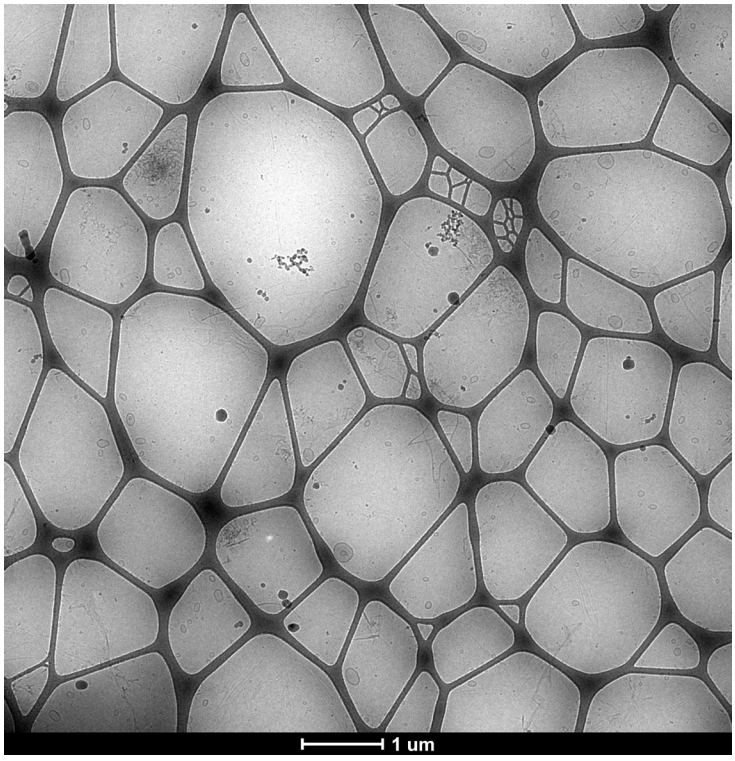


Figure S6.6 Cryo-TEM image of $mPEG_{20}$-*b*-$PCL_{40}$-*b*-$mPEG_{20}$ triblock copolymer self-assembly suspension

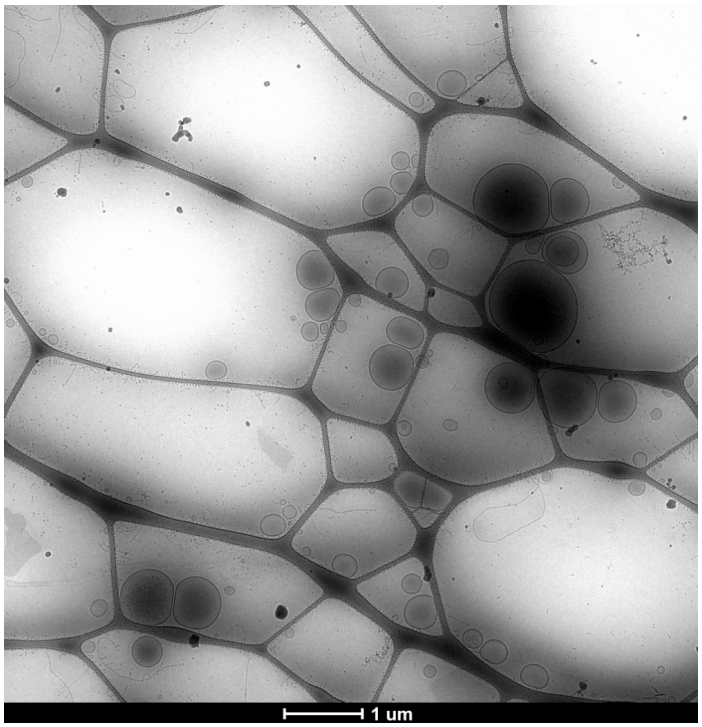


Figure S6.7 Cryo-TEM image of self-assembly suspension of 2 % $NH_2$-$PEG_{43}$-*b*-$PCL_{42}$ diblock copolymer doped into pristine $mPEG_{43}$-*b*-$PCL_{42}$ diblock copolymer

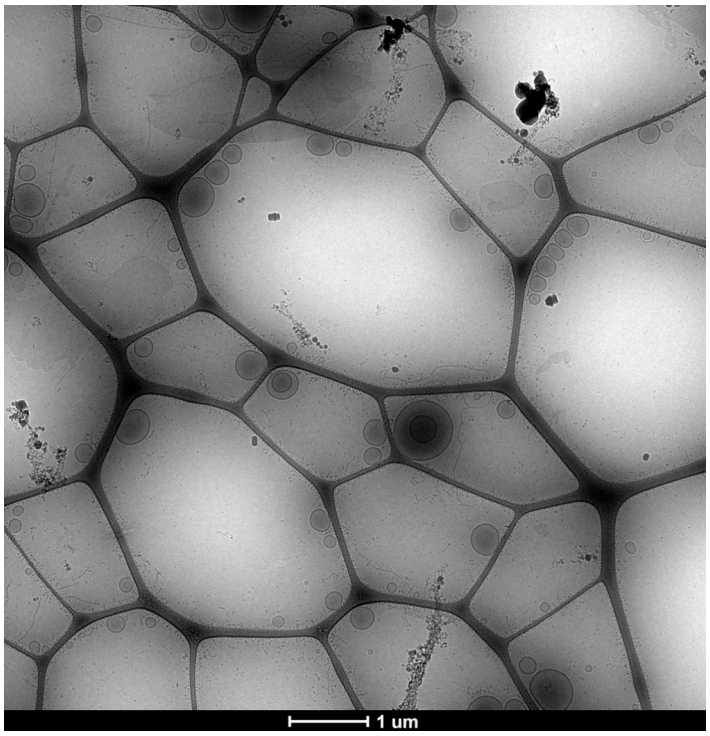


Figure S6.8 Cryo-TEM image of self-assembly suspension of 5 % $NH_2$-$PEG_{43}$-*b*-$PCL_{42}$ diblock copolymer doped into pristine $mPEG_{43}$-*b*-$PCL_{42}$ diblock copolymer

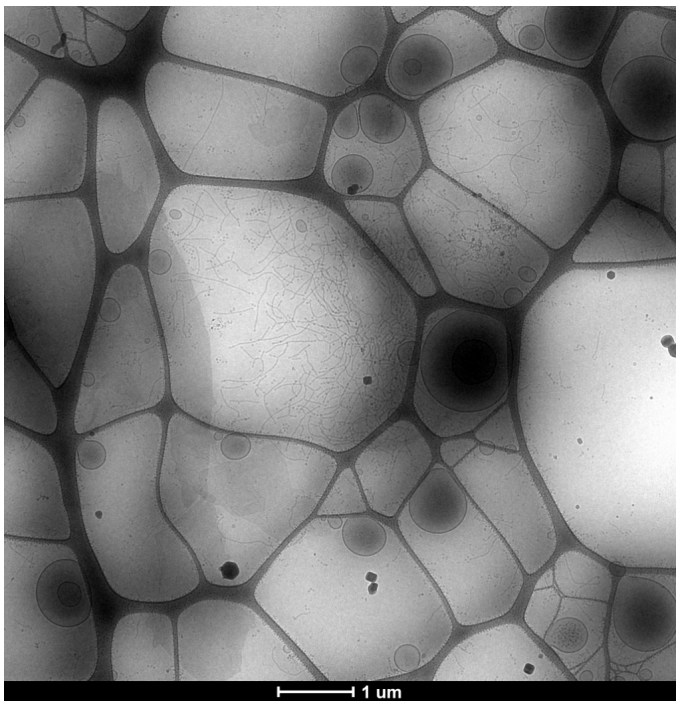


Figure S6.9 Cryo-TEM image of self-assembly suspension of 10 % $NH_2$-$PEG_{43}$-*b*-$PCL_{42}$ diblock copolymer doped into pristine m$PEG_{43}$-*b*-$PCL_{42}$ diblock copolymer

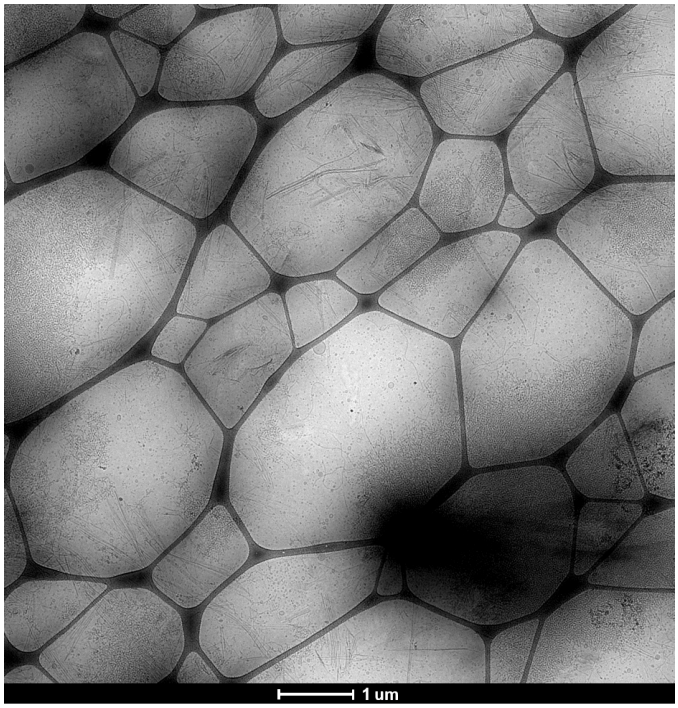


Figure S6.10 Cryo-TEM image of pure $NH_2$-$PEG_{43}$-*b*-$PCL_{42}$ diblock copolymer self-assembly suspension

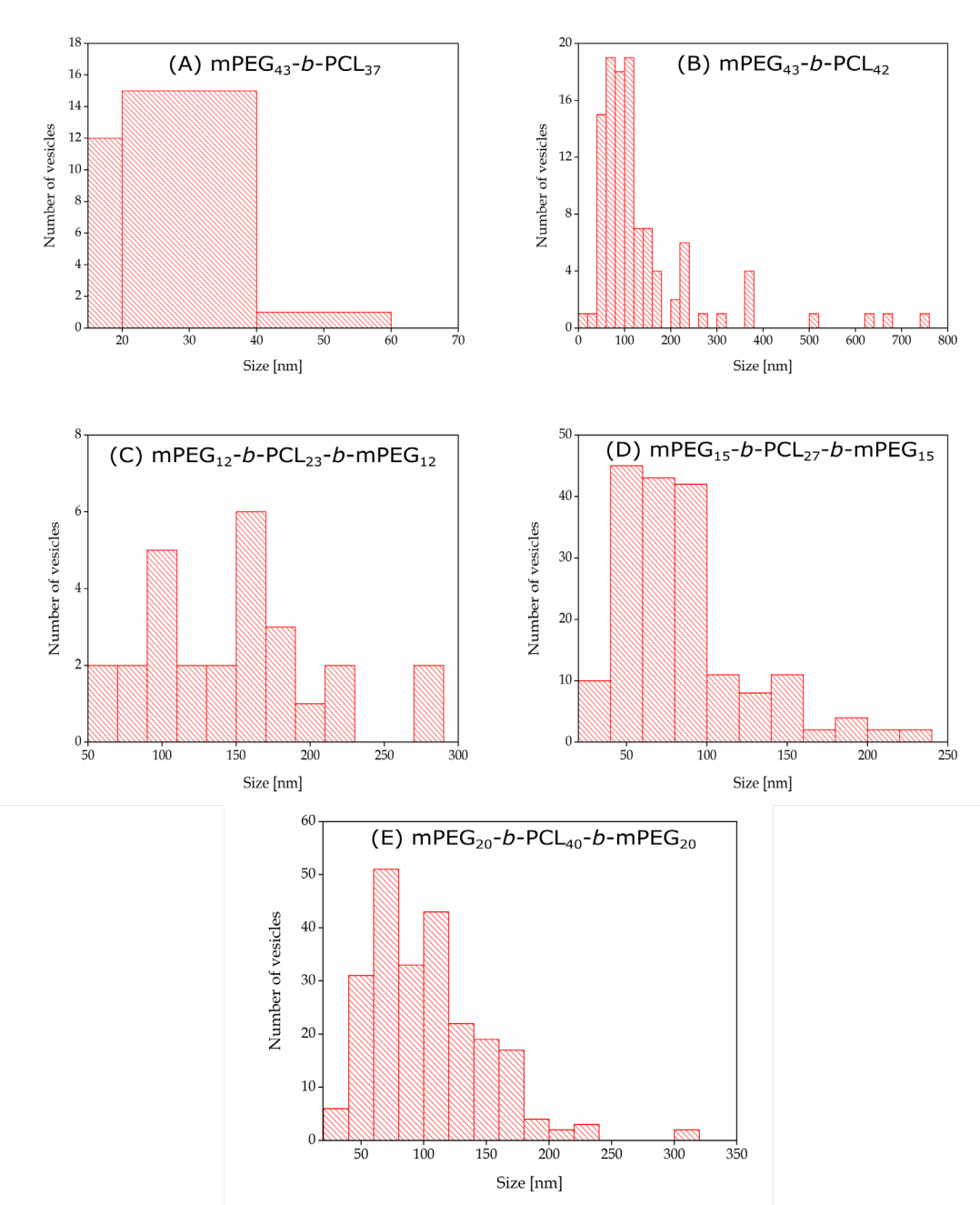


Figure S6.11 Size distribution of the different vesicle suspensions. Size of the vesicles were obtained by analyzing Cryo-TEM images using ImageJ image processing software. Each figure represents number of vesicle species and their corresponding diameter in nm. The diameter was assessed by using a calibrated scale in the software, where the largest distance was taken from one outer edge of the bilayer to the other. Displayed figures are resulting from a single Cryo-TEM image of the same (lowest) magnification (Figure S5.1-S5.2, S5.4-S5.6). Vesicles were picked out by observation with an eye

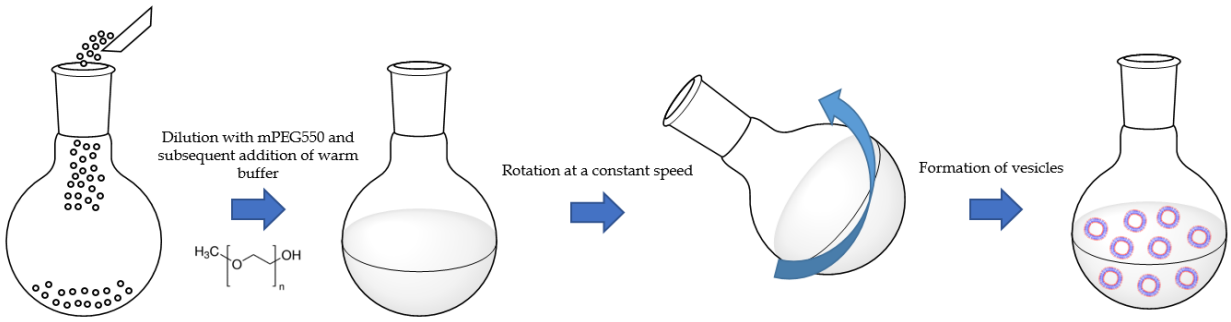


Scheme S1. Vesicle formation with the direct hydration technique. Addition of warm buffer/MiliQ was performed in multiple steps: 1) preheated aqueous media (0.1 mL, 40 °C) was added and rotated at 300 rpm for 30 min, 2) preheated aqueous media (0.2 mL, 40 °C) was added and rotated at 300 rpm for 30 min, 3) preheated aqueous media (0.7 mL, 40 °C) was added and rotated at 300 pm for 30 min

Table S1. Results from 'LINEST' least squares fit from Excel on the natural logarithms of measured membrane thicknesses as a function of the degree of polymerisation

| Parameter | Triblock wall thickness, this work | Wall thickness, reference 69 in main paper |
|---|---|---|
| ln k | -0.648 | -1.35 |
| b | 0.811 | 0.698 |
| Standard Error ln k | 0.826 | 0.340 |
| Standard Error b | 0.244 | 0.080 |
| $R^2$ | 0.917 | 0.927 |

Table S2. $NH_2$-PEG-*b*-PCL doping into pristine mPEG-*b*-PCL

| Amount of PEGME $M_n$ ~ 550, [g] | Amount of $NH_2$-PEG-*b*-PCL stock solution [g][a] | Amount of pristine mPEG-*b*-PCL [g] | $NH_2$-PEG-*b*-PCL wt % (in relation to mPEG-*b*-PCL) |
|---|---|---|---|
| 0.4905 | 0.01 | 0.0495 | 1 |
| 0.4810 | 0.02 | 0.0490 | 2 |
| 0.4525 | 0.05 | 0.0475 | 5 |
| 0.4050 | 0.10 | 0.0450 | 10 |
| 0.3100 | 0.20 | 0.0400 | 20 |

[a]Stock solution of $NH_2$-PEG-*b*-PCL was prepared by dispersing 25.0 mg of such polymer in 475 mg of PEGME (Mn ~ 550 g $mol^{-1}$). In the case where only $NH_2$-PEG-*b*-PCL was used, 50.0 mg of such polymer was mixed with 500 mg of PEGME (Mn ~ 550 g $mol^{-1}$)